Hindawi Publishing Corporation
Advances in OptoElectronics
Volume 2011, Article ID 376369, 9 pages
doi:10.1155/2011/376369

Research Article

Change of Dye Bath for Sensitisation of Nanocrystalline TiO_2 Films: Enhances Performance of Dye-Sensitized Solar Cells

Malapaka Chandrasekharam,[1] Ganugula Rajkumar,[2] Chikkam Srinivasa Rao,[1] Paidi Yella Reddy,[2] and Mannepalli Lakshmi Kantam[1]

[1] *Inorganic and Physical Chemistry Division, Indian Institute of Chemical Technology, Uppal Road, Tarnaka, Hyderabad 500607, India*
[2] *Aisin Cosmos R and D Co. Ltd, Indian Institute of Chemical Technology, Uppal Road, Tarnaka, Hyderabad 500607, India*

Correspondence should be addressed to Malapaka Chandrasekharam, csmalapaka@yahoo.com

Received 24 April 2011; Accepted 25 May 2011

Academic Editor: Surya Prakash Singh

The photovoltaic performance of the heteroleptic **H**102 and **HRD**2 sensitizers was measured in DSSC and compared with that of reference N719 under similar fabrication and evaluation conditions. The Dye-Sensitised TiO_2 electrodes were prepared by staining the electrodes in ethanol bath and 1/1 v/v acetonitrile/*tert*-butanol (binary liquid) mixture bath separately and the DSSCs based on these sensitizers show that the change of dye bath from ethanol to the binary liquid mixture enhances the photocurrent action spectrum and solar-to-electricity conversion efficiencies, (η). Using ethanol for sensitisation of TiO_2 electrodes, the efficiencies obtained for **H**102, **HRD**2 and N719 are 4.31%, 4.62%, and 5.46%, respectively, while in binary liquid mixture bath, the corresponding values are enhanced to 5.89%, 4.87%, and 7.23%, respectively, under comparable conditions.

1. Introduction

Among organic photovoltaic cells Dye-Sensitised Solar Cells (DSSCs) are known to be very promising due to their high efficiency and low-cost technology for the conversion of light energy into electricity [1–6]. The sensitizer is one of the most important elements that influence the overall performance of the DSSC. Ruthenium(II) polypyridyl complexes have wide applications as the most efficient sensitizers, because of the intense metal-to-ligand charge transfer (MLCT) transition exhibited in the visible region. Another important advantage of ruthenium sensitizers is their relative stability in oxidized and reduced forms and the ease of tuning their spectral, photo-physical, and electrochemical properties by bringing about structural changes in the bipyridyl ligand [7–13]. The most efficient test cell DSSC has been developed by Grätzel and coworkers by employing *cis*-dithiocyanato bis(4,4′-dicarboxy-2,2′-bipyridine)ruthenium(II) (known as N3 dye). The solar-to-electricity conversion efficiency up to 11% has been reached with N3 under AM 1.5 G on irradiation with a nanostructured TiO_2 electrode and iodine redox electrolyte [14–17]. Usually anchoring ligands and ancillary ligands are incorporated in the metal-complex sensitizers so that anchoring ligands are responsible for grafting the dye on the semiconductor surface and providing a medium for electron injection from the excited state of the sensitizer to the conduction band of the semiconductor, whereas ancillary ligands have a scope for structural variations by chemical modifications for tuning the overall properties of the complexes. To ensure fast and efficient electron injection, one of the energy levels of the dye, lowest unoccupied molecular orbital (LUMO), must be higher than that of the TiO_2 conduction band edge. To generate the neutral dye molecule, the highest occupied molecular orbital (HOMO) must align below the oxidation potential of the redox mediator. An understanding of the relative positions of the energy levels of the dye adsorbed on the semiconductor is useful for explaining the efficiency of electron transfer from the excited dye to the semiconductor and device performance.

Modification of the dye is one of the strategies to improve the performance of DSSCs. A possible way of finding new metal-complex sensitizers with good conversion efficiencies was investigated by attaching variety of π-conjugated group to the ancillary ligand. Replacement of one of the H2dcbpy anchoring ligands with a highly conjugated ancillary ligand results in an increase of extinction coefficients and therefore the photocurrent density of the DSSCs [9, 18–20]. As a part of our continued program on synthesis of new materials and their evaluation in DSSC performance, we have synthesized various sensitizers especially extended π-conjugated bipyridyl-based ruthenium(II) complexes for efficient and long-term durability DSSCs [21–24]. We have also demonstrated in our laboratory that extended π-conjugation with styryl group on the ancillary bipyridine increases the molar extinction coefficient of the ruthenium sensitizer but reduces the solubility, whereas extension of conjugation by directly electronically connecting the aryl groups on the ancillary bipyridines increases solubility and also improves overall photovoltaic performance of the DSSC test cells significantly [25–27]. Effect of different dye baths and dye-structures on the performance of dye sensitized solar cells based on triphenylamine organic dyes has been reported recently [28]. In this paper we report the photovoltaic studies of three sensitizers in DSSCs, wherein we have employed two different dye baths one in ethanol and the other is a mixture of 1/1 v/v acetonitrile/*tert*-butanol mixture to sensitise the TiO_2 electrodes. Out of the various solvents, the sensitizers exhibited high molar extinction coefficient in both the solvent systems, which are considered for staining the TiO_2 electrodes. We have examined the sensitizers **HRD**2 (*cis*-Ru(4,4′-bis(2,4,6-trimethylstyryl)-2,2′-bipyridine-2,2′-bipyridine) (Ln) $(NCS)_2$) and **H**102 (*cis*-Ru(4,4′-dimesityl-2,2′-bipyridine)(Ln)$(NCS)_2$), where Ln = 4,4′-dicarboxylic acid-2,2′-bipyridine) to study the influence of dye baths on the photovoltaic performance of DSSCs and the photovoltaic characteristics were compared with reference cell, **N**719 constructed under comparable conditions.

2. Results and Discussions

2.1. Synthesis. Synthetic route for the preparation of **HRD**2 and **H**102 sensitizers are shown in Scheme 1. The tetraethyl 2,2′-bipyridine-4,4′-diylbis(methylene)diphosphonate was prepared in accordance to the reported procedure [21] and the ancillary bipyridine ligand, 4,4′-bis(2,4,6-tri methylstyryl)-2,2′-bipyridine (**L**1) was prepped by reacting 2,4,6-trimethylbenzaldehyde with phosphonate derivative under Wittig conditions, while 4,4′-dimesityl-2,2′-bipyridine (**L**2) was prepared from mesitylboronic acid and 4,4′-dibromo-2,2′-bipyridine under palladium catalysed Suzuki conditions. The reaction of the ligands (**L**1/**L**2) with dichloro (*p*-cymene) ruthenium(II) dimer in presence of refluxing DMF afforded chloro (*p*-cymene) ruthenium bipyridyl complex intermediate, which on further reaction with 2,2′-bipyridine-4,4′-dicarboxylic acid in presence of excess NH_4NCS resulted in formation of **HRD**2 and **H**102 complexes, respectively. The crude compounds were purified on Sephadex LH 20 column chromatography. The use of TBA was necessitated during the column purification of **HRD**2 sensitizer that indicates its relatively lower solubility in organic solvents. This is expected due to ethenyl spacer's introduction in dye molecule, which reduces the solubility as compared to the corresponding analog with excluded ethenyl spacers. **N**719 complex was synthesized in accordance to the reported procedure.

*2.1.1. Synthesis of 4,4′-bis-[2-(2,4,6-trimethyl-phenyl)-vinyl]-[2,2′]-bipyridyl (**L**1).* Sodium hydride 60% (184 mg, 7.625 mmol) was washed with dry hexane (3 times) and THF (40 mL) was added. To this suspension a THF solution of bipyridine diphosphonate (700 mg, 1.535 mmol) was added and the resulting mixture was stirred at room temperature for a period of 30 minutes. Then the 3,5 di-*tert* butyl benzaldehyde (0.652 mL, 3.375 mmol) dissolved in THF was added dropwise at room temperature with stirring. The reaction mixture was refluxed for 12 hours and the mixture was allowed to cool to room temperature and extracted with DCM and evaporated. After drying and evaporation, the residual was purified on silica gel column chromatography using DCM-MeOH (9 : 1) as eluent. This compound was characterized by NMR spectroscopy. White solid. yield 50%, ^{1}HNMR (300 MHz, 25°C, $CDCl_3$) 2.35 (s, 18H), 6.58 (d, 1H), 6.62 (s, 4H), 7.25 (s, 2H), 7.31 (d, 1H), 8.63 (d, 2H), 8.71 (d, 2H). Chemical formula $C_{32}H_{32}N_2$, ESIMS: Calcd for M.wt 444, found: 444.

*2.1.2. Synthesis of 4,4′-dimesityl-2,2′-bipyridine (**L**2).* In a 25 mL one-necked round bottom flask equipped with a condenser were placed mesityl boronic acid (250 mg, 1.528 mmol), barium hydroxide octa-hydrade (1.5 g, 4.77 mmol) and palladium tetrakis triphenyl phosphine (146 mg, 0.127 mmol). The reaction flask was evacuated and filled with nitrogen gas, then 1,4-dioxane/water (v/v, 3 : 1, 8 mL) and 4,4-dibromo-2,2′-bipyridine (200 mg, 0.636 mmol) were added. The reaction mixture was refluxed for 24 hours under nitrogen gas and cooled to room temperature. The dioxane was removed and the contents were poured into dichloromethane, the precipitate formed was removed by filtration through filter paper and the organic layer was washed with 1.0 M NaOH aqueous solution, and dried over sodium sulphate. After rotoevaporation of dichloromethane under a reduced pressure, the resulting residue was diluted with a small quantity of methanol. The precipitate formed was immediately filtrated, dried, and purified by column chromatography on silica gel with dichloromethane/methanol mixture (9/1) as eluent to afford the ligand **L**2. (329 mg, 55% yield); ^{1}H NMR (in $CDCl_3$) 2.10 (s, 6H), 2.38 (s, 3H), 6.99 (s, 2H), 7.16 (d, 1H), 8.31 (s, 1H), 8.72 (d, 1H); ESI-MASS: $C_{28}H_{28}N_2$ (m + 1) = 393 (100%).

2.1.3. Synthesis of Ru(II) Complexes (Representative Procedure). Compound **L**1/**L**2 (0.902 mmol) and dichloro-(*p*-cymene)-ruthenium(II) dimmer (276 mg, 0.451 mmol) in DMF were heated at 60°C for a period of 4 hours under nitrogen in the dark. Subsequently, 4,4′-dicarboxylic

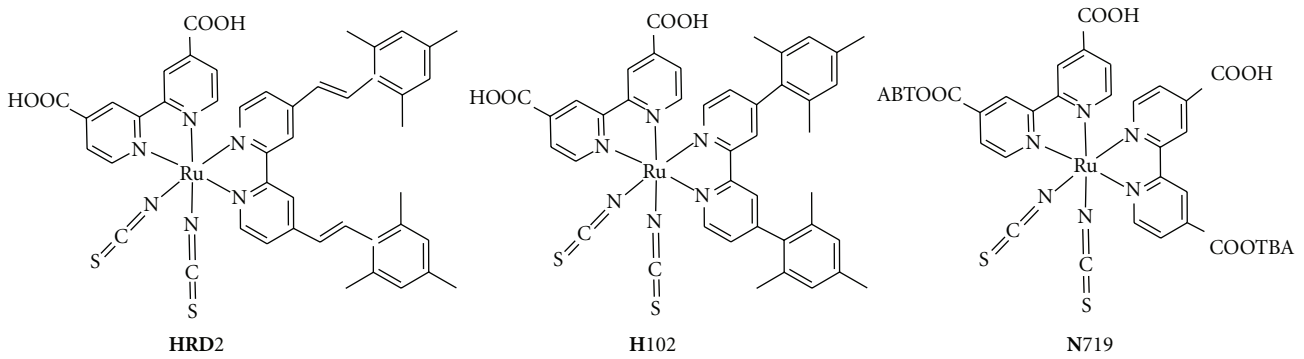

Figure 1: Structures of new heteroleptic polypyridyl ruthenium(II) sensitizers.

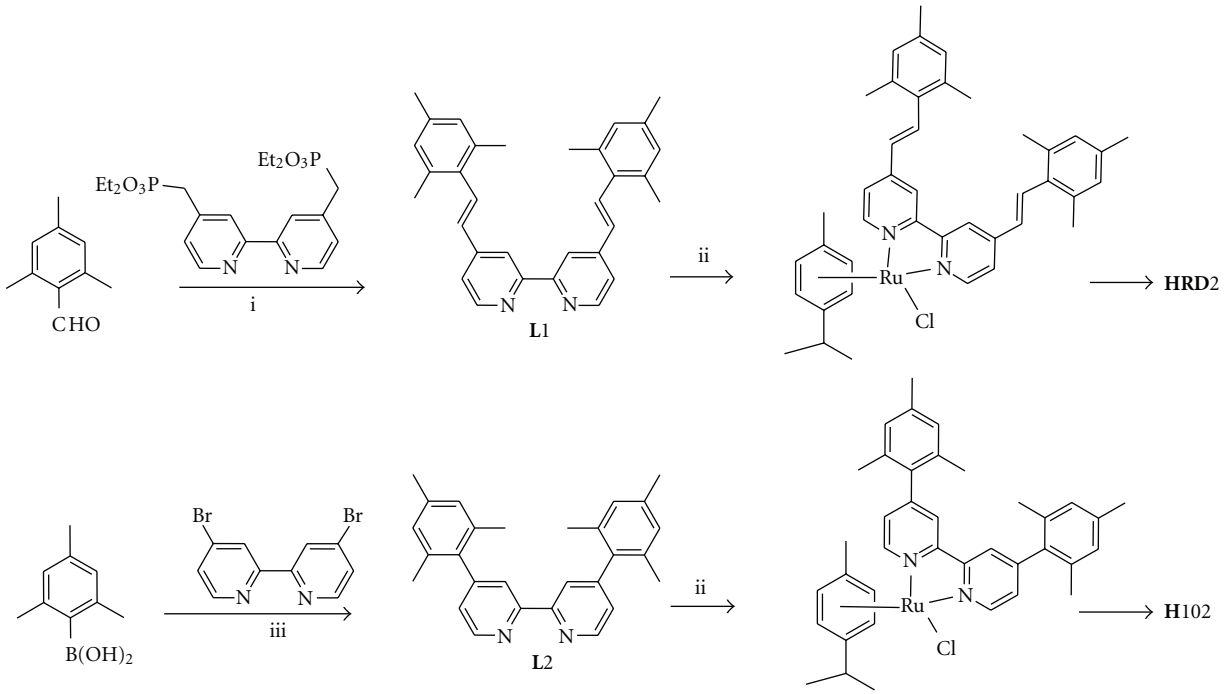

Scheme 1: Synthetic route for **HRD**2 and **H**102 sensitizers; (i) NaH-THF, reflux for 12 hours (yield-55%). (ii) Ru-*p*-cymene complex, 2,2′-bipyridine-4,4′-dicarboxylic acid, NH_4NCS, DMF, reflux for 12 hours. (iii) $Ba(OH)_2 \cdot 8H_2O$, $Pd(PPh_3)_4$, Dioxane: H_2O, reflux for 24 hours.

acid-2,2′-bipyridine (220 mg, 0.902 mmol) was added and the reaction mixture was heated to 140°C for another 4 hours. To the resulting dark green solution was added solid NH_4NCS (2.060 g, 22.06 mmol) and the reaction mixture was further heated for 4 hours at 140°C. After rotoevaporation of DMF, water (250 mL) was added to get precipitate. The purple solid was filtered off, washed with water and ether, and then dried under vacuum. The crude compound was dissolved in methanol and dichloromethane and purified by column chromatography on Sephadex LH-20 with methanol/dichloromethane (TBA methanol in case of **HRD**2) mixture (3/2) as eluent to afford ruthenium complexes (see Figure 1).

***HRD**2 (yield 65%); ^{1}H-NMR (300 MHz, 25°C, CD_3OD) δ [ppm].* 0.90 to 3.4 (m, 54H), 6.65 (d, 1H), 6.82 (d, 1H), 6.90 (s, 2H), 6.98 (s, 2H), 7.20 (d, 1H), 7.35 (d, 1H), 7.50 (d, 1H), 7.56 (d, 1H), 7.65 (d, 1H), 7.78 (d, 1H), 7.83 (d, 1H), 8.09 (d, 1H), 8.4 (s, 1H), 8.55 (s, 1H), 8.87 (s, 1H), 8.96 (s, 1H), 9.35 (d, 1H), 9.46 (d, 1H); ESI-MS: 1147.

***H** 102 (65% yield); ^{1}HNMR ($CDCl_3$ + CD_3OD) δ [ppm].* 1.90 (s, 3H), 2.07 (s, 3H), 2.23 (s, 3H), 2.26 (s, 3H), 2.31 (s, 3H), 2.40 (s, 3H), 6.91 (s, 1H), 6.97 (s, 1H), 6.99 (d, 1H), 7.08 (s, 1H), 7.55 (d, 1H), 7.67 (d, 1H), 7.78 (s, 1H), 7.90 (d, 1H), 8.00 (s, 1H), 8.15 (s, 1H), 8.31 (d, 1H), 9.79 (d, 1H), 8.89 (s, 1H), 9.02 (s, 1H), 9.58 (d, 1H); ESI-MASS: $C_{42}H_{36}N_6O_4RuS_2$ (m + 1) = 853 (100%).

2.2. Electronic Absorption, Emission, and Electrochemical Properties. The electronic absorption spectra of the equimolar solutions of 4,4′-bis(2,4,6-trimethylstyryl)-2,2′-bipyridine (**L**1) shows increased light harvesting ability as compared to 4,4′-dimesityl-2,2′-bipyridine (**L**2), which is

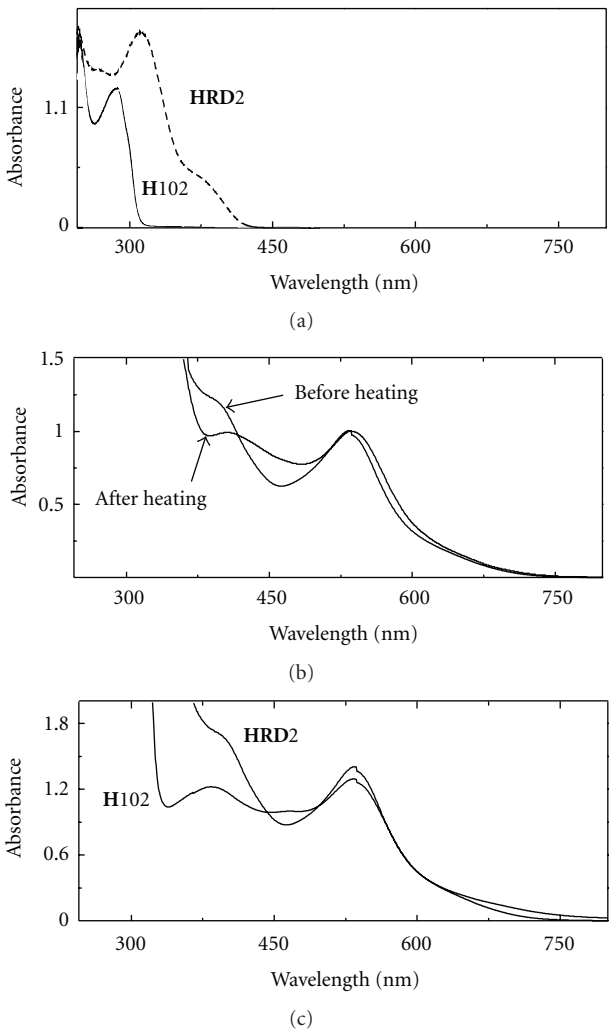

Figure 2: Equimolar electronic absorption spectra of 4,4′-bis(2,4,6-trimethylstyryl)-2,2′-bipyridine (**L**1) and 4,4′-dimesityl-2,2′-bipyridine (**L**2) in $CHCl_3$; (b) the absorption spectra of **HRD**2 in DMF; (c) normalized absorption spectra of **HRD**2 and **H**102 complexes in DMF.

expected due to extension of π-conjugation and is akin to the molecular cosensitization for efficient panchromatic DSSC sensitizers [29] (Figure 2(a)). In order to know the tendency of these sensitizers at high concentrations of the dye solutions employed for staining the TiO_2 electrodes, the absorption spectra of **HRD**2 recoded at 0.1 mM of dye solution in DMF showed one charge transfer band in long wavelength region with a weak shoulder type high-energy band at 373 nm (Figure 2(b)). As compared to this, the absorption pattern recorded after heating the dye solution at around 50°C was changed, in which a clear high-energy band with bathochromic. Shift was observed (Figure 2(c)). To explain the observation, the absorption studies carried out with the ancillary ligands, **L**1 and **L**2 showed absorption bands at 286 and 311 nm, respectively, with a small shoulder type band at 385 nm for **L**1, which was observed disappearing on heating (Figure 2(b)). It seems that this absorption band could be due to the presence of molecular aggregation in **L**1, which was suppressed due to increased solvation upon heating. Having similar oligophenyls in **L**1, the absence of such phenomenon in the absorption spectrum of **H**102 indicates that the presence of ethenyl spacers favours aggregation. The disappearing of the band at 373 nm in **HRD**2 complex on heating could be also probably due to the presence of such aggregation. This indicates the necessity of heating the dye solution of **HRD**2 before staining the TiO_2 electrodes and proceeding further to fabricate DSSC cells.

The electrochemical properties of **HRD**2 and **H**102 dyes scrutinized by cyclic voltammetry using an electrolyte of tetrabutyl ammonium perchlorate (0.1 M in acetonitrile) and ferrocene as an internal standard at 0.42 V versus SCE [25–27]. The oxidation potentials for **HRD2** and **H**102 sensitizers were 0.80 and 0.816 V versus SCE, respectively, while the reduction potentials were −0.758 and −0.94 V versus SCE, respectively. The more positive potentials of these sensitizers, relative to I^-/I_3^- redox couple in the electrolyte, provide a large thermodynamic driving force for the regeneration of the dyes by iodide. The corresponding standard potentials ($\phi^0(S+/S^*)$) for these sensitizers were −1.13 and −1.019 V versus SCE are more negative (or higher in energy) than the conduction band edge of TiO_2 providing a thermodynamic driving force to inject electron from the dye to TiO_2.

Although **HRD**2 showed relatively increased molar extinction coefficient as compared to **H**102, the molecular diameter increases with increasing the π-conjugation length affecting the solubility of sensitizers, which inturn influence the molecular aggregation of dye molecules in solution. This indirectly affects the packing densities of dye molecules on TiO_2 electrodes and thereby photovoltaic performance. In order to see the influence of geometrical structure and the type of dye bath on staining TiO_2 electrodes, TiO_2 films of 7.0 μm thick (18 NRT layered) were stained in the dye solutions of 0.3 mM concentration prepared separately in ethanol and in the binary liquid mixture for a period of 16 hours under dark. Prior to the staining, the dye solutions of **HRD**2 are heated at 50°C for around 5 hours. The absorption spectra of **HRD2** and **H**102 sensitized TiO_2 films were recorded and were compared with that of **N**719 (Figures 3(a) and 3(b)). The measurements indicate that the dye molecules are anchored on TiO_2 surface and the spectra of mesoporous TiO_2 films stained in ethanol bath seem to be more or less similar in trend with those obtained using the binary liquid mixture bath. But as compared to staining in ethanol bath, the little increased film absorbance ratios in the binary liquid mixture was initially thought of better solubility of the complexes. To examine the influence of different oligophenyl substitutions on solubility of **HRD**2 and **H**102 and their impact on film absorbance ratio, the absorption measurements were performed as function of wavelength in ethanol and in the binary liquid mixture. The electronic equimolar absorption spectra recorded in ethanol are similar in pattern as compared to those recorded in

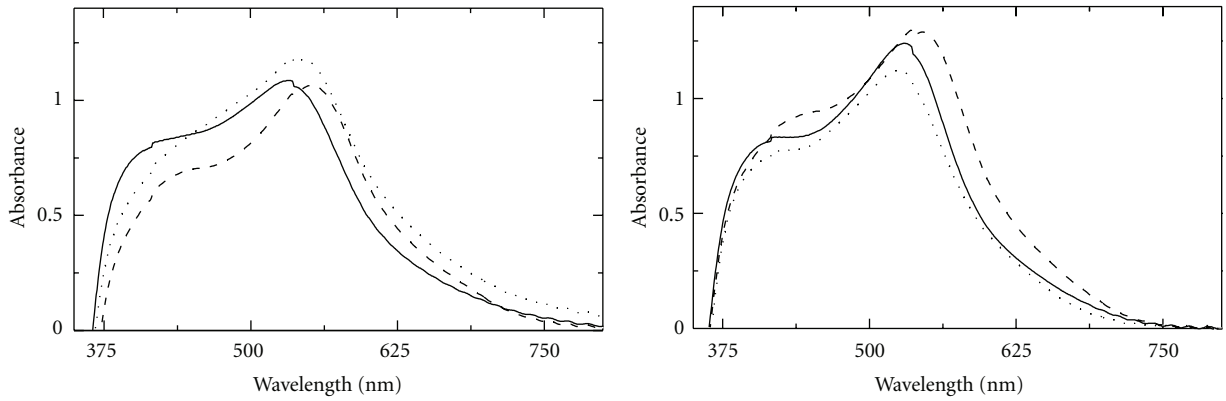

FIGURE 3: Absorption spectra of dye-sensitized 7.0 μm thick mesoporous titanium films (a) in ethanol bath; **HRD**2 (—), **H**102 (----), and **N**719 (· · · ·); (b) binary liquid mixture bath; **HRD**2 (· · · ·), **H**102 (—), and **N**719 (----) (calculated error obtained in maximum absorbance is ±2.5%).

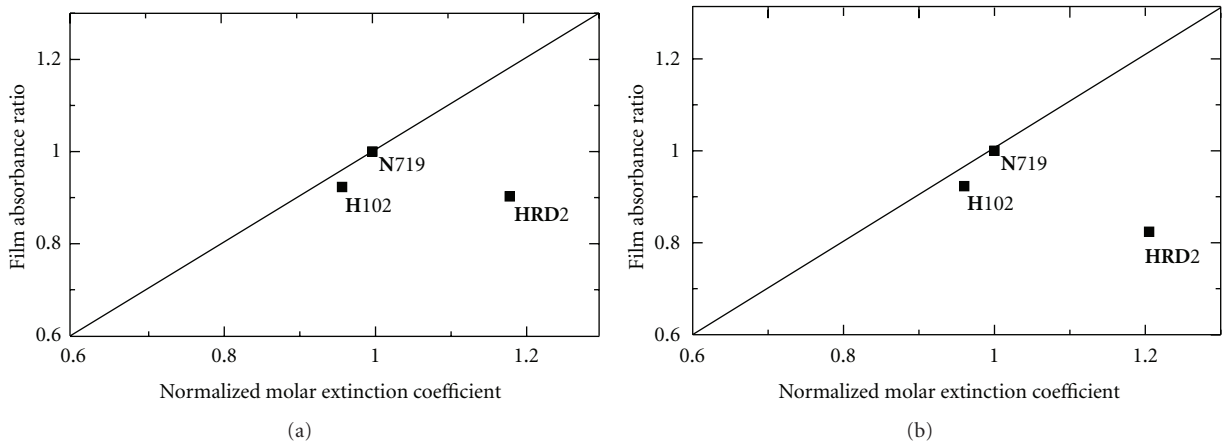

FIGURE 4: Film absorbance ratio versus normalized molar extinction coefficients of the sensitizers anchored on 7.0 μm thick mesoporous titanium films (a) ethanol bath (b) 1/1 v/v acetonitrile/*tert*-butanol mixture bath (here the low-energy maximum absorbance of **HRD**2 and **H**102 sensitizers are normalized relative to that of **N**719). An average of three film absorbencies of three different mesoporous TiO_2 films gave error below ±2.5%.

the binary liquid mixture indicating that these **HRD**2 and **H**102 dyes are dissolving in both the solvent systems with equal ease. It can be concluded from the above observation that the slight disparity in the film absorbance ratio could not be due to the difference in the solubility of these sensitizers.

To compare the anchoring pattern and surface morphology of these dye sensitised TiO_2 films, the absorbance maxima of low-energy absorption bands of **HRD**2 and **H**102 sensitizers are normalized by the corresponding absorbance maxima of **N**719, while their molar extinction coefficients are normalized by the molar extinction coefficient of **N**719. Figure 4(a) shows the film absorbance of dye sensitized TiO_2 films stained in ethanol bath plotted against the normalized molar extinction coefficients, while Figure 4(b) corresponds to that obtained using the binary liquid mixture bath. The hypothetical diagonal line in both the plots is based on the calculated linear relationship between the film absorbance and normalized molar extinction coefficient of low-energy absorption bands.

The film absorbance ratio of **HRD**2 and **H**102 sensitizers falling below to the diagonal line indicates the lower packing densities of these sensitizers on the TiO_2 surface relative to **N**719 sensitizer. The lowest packing density of these sensitizers could be probably due to relatively increased molecular diameter, since the measurements reported earlier on the surface coverage of sensitizer on titania estimated through ICP-OES analysis augment with the calculated coverage of ruthenium(II) polypyridyl sensitizers**.** The film absorbance versus molar absorptivities drawn by staining the TiO_2 films in ethanol bath and in the binary liquid mixture bath are similar in trend and indicate that changing the dye bath from ethanol to the binary liquid mixture for loading of sensitizers on TiO_2 surface has no significant

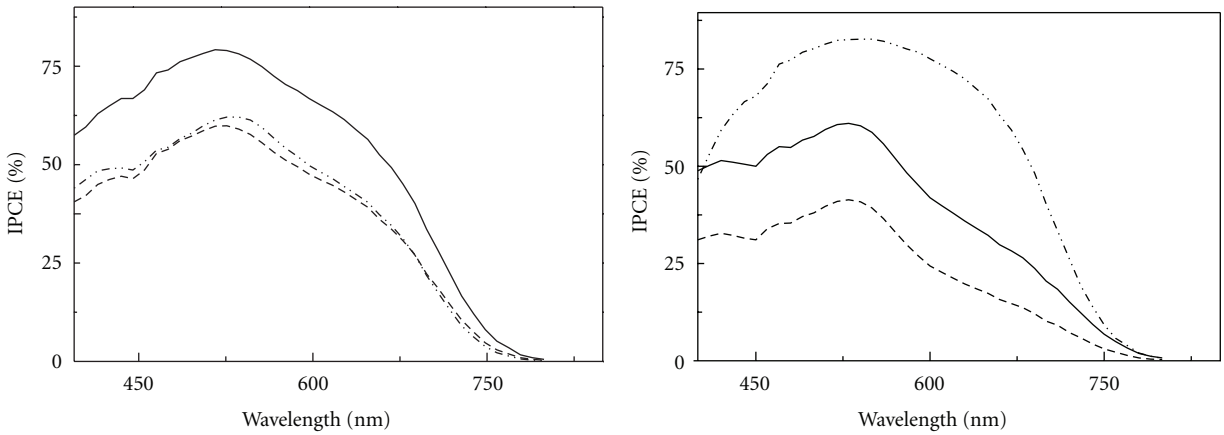

FIGURE 5: Photocurrent action spectra of devices fabricated by staining TiO_2 electrodes from dye baths (a) ethanol, (b) 1/1 v/v acetonitrile/*tert*-butanol mixture bath (**HRD**2 (----), **H**102 (· · · · ·), and **N**719 (—)).

influence on packing densities of these **HRD**2 and **H**102 sensitizer molecules relative to **N**719. The differences that have seen in these plots could be a result of substitution of one of the bipyridyl moieties of **N**719 by different ancillary bipyridyl ligands, 4,4′-bis(2,4,6-trimethylstyryl)-2,2′-bipyridine and 4,4′-dimesityl-2,2′-bipyridine, in which the intra $\pi \rightarrow \pi^*$ transitions of these ancillary ligands influence on their contribution for high/low-energy MLCT absorption bands and also by the change in the structural morphology of the sensitizers. Although the change of dye bath from ethanol to the binary liquid mixture has not shown any major influence on their film absorbance ratios of **HRD2** and **H**102 sensitizers, certainly the physical state of these sensitizer molecules in ethanol and in the binary liquid mixture are not to be the same as the recent reports reveal that in the combination of liquid mixtures, few molecular associations are influenced by hydrogen bonding through dipole-dipole interactions [29]. We believe that the variation in the solvents used in dye baths also influence on delivery of the dye molecules and the pattern of dye molecules sitting on the surface TiO_2 during the anchoring phenomenon and ultimately lead to influence the overall light to electricity conversion efficiencies.

2.3. Photovoltaic Performance. The DSSCs were fabricated using dye sensitized 0.54 cm^2 TiO_2 electrodes in combination with I^-/I_3^- redox couple electrolyte, (**E**01) containing 0.05 M I_2, 0.1 M LiI, 0.6 M 1,2-dimethyl-3-*n*-propylimidazolium iodide, 0.5 M 4-*tert*-butylpyridine in acetonitrile solvent. The fabrication of DSSC test cells are followed in accordance to earlier reported procedure [22]. Reference DSSCs were fabricated and evaluated under identical conditions using **N**719 sensitizer. Incident photon-to-current conversion efficiency spectra were measured using illumination from a 150 W Xe lamp/grating monochromator calibrated ithilicon photodiode (traceable (5% to NBS)). The current-voltage characteristics of the cells were measured using a xenon arc solar simulator (ELLSOL 1000, model SVX 1450) with an AM 1.5 spectral filter, and the intensity was adjusted to provide 1 Sun (100 mW cm^{-2}) using a calibrated GaAs solar cell. Based on *I*-*V* curve, the fill factor (ff) is defined as $\text{ff} = (I_{\max} \times V_{\max})/(I_{sc} \times V_{oc})$, where $I_{\max}$ and $V_{\max}$ are photocurrent and photovoltage for maximum power output ($P_{\max}$), I_{sc} and V_{oc} are the short-circuit photocurrent and open-circuit photovoltage, respectively. The overall energy conversion efficiency (η) is defined as $\eta = (I_{sc} \times V_{oc} \times \text{ff})/P_{in}$, where P_{in} is the power of incident light. The incident photon-to-current conversion efficiencies (IPCEs) of DSSCs constructed based on **HRD**2 and **H**102 sensitizers are plotted as function of excitation wavelength and their IPCE spectra were compared with that of **N**719 cell.

Figures 5(a) and 5(b) presents the typical photocurrent action spectra of the DSSCs fabricated from TiO_2 electrodes sensitized by dye baths of ethanol and the binary liquid mixture, respectively. The maximum IPCE observed for all these dyes are within the spectral range of 450–600 nm. With the combination of **E01** as an electrolyte, the DSSCs constructed based on **H**102 sensitizer exceeds IPCE values of 60%. However, change of dye bath from ethanol to the binary liquid mixture enhanced IPCE value up to 80%, considering the light absorption and scattering loss by the conducting glass, the maximum efficiency for absorbed photon-to-collected electron conversion efficiency (APCEs) of **H**102 sensitizer is almost close to unity. The enhancement in IPCE value and the broadened IPCE spectra obtained with change of dye bath suggests that the solvent composition is also important to obtain high performance and particular attention has to be paid to the molecular adsorption morphology of dyes or and delivery of sensitizer molecules on TiO_2 electrodes for the best device efficiencies.

One of the factors responsible for this improvement in IPCE spectra observed on changing the dye baths could be initially thought of better solubility of these sensitizers in the binary liquid mixture, in which acetonitrile has higher dipole moment (3.92 D) as compared to ethanol (1.69 D).

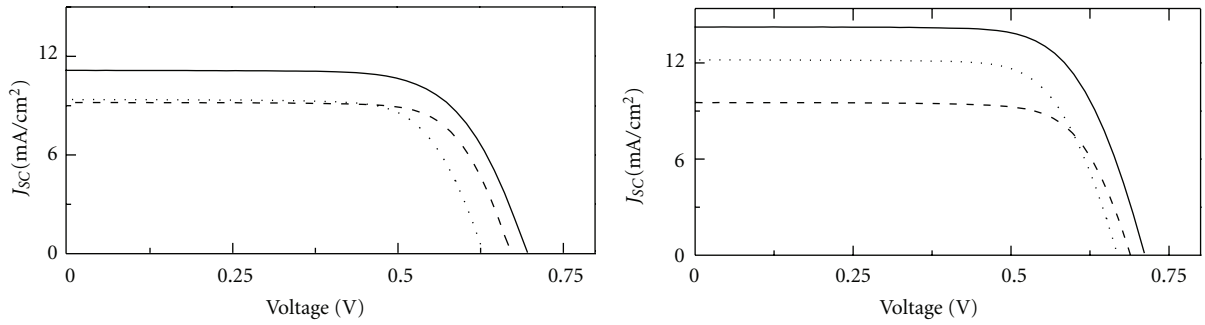

Figure 6: J-V characteristics of DSSC devices of **HRD**2 (----), **H**102 (· · · · ·), and **N**719 (—) fabricated by staining TiO_2 electrodes from dye bath (a) ethanol (b) 1/1 v/v acetonitrile/*tert*-butanol mixture measured under the irradiance of AM 1.5 G sunlight of 100 mW cm^{-2}.

The other possibility could be relatively higher packing densities of these sensitizer molecules on nanocrystalline TiO_2 electrodes, when the binary liquid mixture was employed as dye bath. But the absorption measurements of **HRD**2 and **H**102 sensitizers carried out separately in the binary liquid mixture showed molar extinction coefficients more or less similar to those obtained in ethanol medium indicating negligible influence on solubility of these sensitizers. Even the film absorbance of **HRD**2 and **H**102 sensitizers adsorbed on TiO_2 films plotted against the molar extinction coefficients show a similar trend indicating similar packing densities of these sensitizers on mesoporous TiO_2 films irrespective of the solvent employed in dye bath. This shows that the improvement in IPCE could not be due to the difference in the quantities of **HRD**2 and **H**102 sensitizers adsorbed on TiO_2 electrodes.

Figures 6(a) and 6(b) show J_{sc}-V curves of DSSC devices recorded under irradiance of AM 1.5 G full sunlight. The open-circuit photo voltages (V_{oc}), short-circuit photocurrent densities (J_{sc}), fill factors (ff), and the corresponding solar-to-electrical energy conversion efficiencies (η) for each dye-sensitized solar cell are listed in Table 1. Keeping in mind the importance of molecular-scale interface engineering, CDCA was employed as coadsorbent (at molar ratio of sensitizer/CDCA as1/3) in the staining solution to improve the device efficiencies.

HRD2 and **H**102 sensitized solar cells yield overall conversion efficiencies of 5.89 and 4.87%, respectively, in binary liquid mixture, while they exhibited 4.31 and 4.62%, respectively, in ethanol. Under comparable conditions, **N**719 sensitize solar cell gave 7.26% in binary liquid mixture, while 5.46% in ethanol. **H**102 sensitizer exhibited lower J_{sc} but higher V_{oc} values resulting in a net decrease in the efficiency as compared to **N**719. But comparing sensitisation in ethanol dye bath, cells constructed based on corresponding binary liquid mixture dye bath sensitized TiO_2 electrodes exhibited higher J_{sc} and V_{oc} and ultimately higher device efficiencies. From the plots of film absorption versus molar absorptivities, there is no much change in the film absorbance ratios, but the overall increase in IPCE spectra of these sensitizers enhance J_{sc} values. In case of **HRD**2 dye, the photovoltaic characteristics of DSSCs, fabricated from TiO_2 electrodes sensitized in dye baths of the binary liquid mixture and ethanol, are almost similar.

Table 1: Detailed photovoltaic parameters of DSSCs fabricated by TiO_2 electrodes sensitized in (a) ethanol bath (b) 1/1 v/v acetonitrile/*tert*-butanol mixture bath.

	Sensitizer	J_{sc} (mA/cm^2)	V_{oc} (mV)	ff	η (%)
(a)	H102	9.38	0.63	0.73	4.31
	HRD2	9.19	0.67	0.75	4.62
	N719	11.15	0.70	0.70	5.46
(b)	H102	12.19	0.67	0.72	5.89
	HRD2	9.53	0.69	0.74	4.87
	N719	14.25	0.72	0.71	7.23

Short-circuit photocurrent density (J_{sc}), open-circuit photovoltage (V_{oc}), fill factor (ff). The electrolyte composition is as follows: **E01**: containing 0.05 M I_2, 0.1 M LiI, 0.6 M 1,2-dimethyl-3-*n*-propylimidazolium iodide, 0.5 M 4-*tert*-butylpyridine in acetonitrile solvent.

It is interesting to note that the higher efficiency (η) value obtained for DSSC based on **H**102 dye, which has the lowest light absorption capability relative to **HRD**2. The reason for this could be the absence of π-conjugation and adoption of suitable electron donors "three methyl groups at suitable positions" in the ancillary ligand. We assume that the absence of ethenyl spacers in **H**102 make the sensitizer free from cis trans-isomerisation observed in **HRD**2, which may lead to self-quenching and reducing η-value of the devices.

3. Conclusions

In summary, the influence of dye baths for staining the TiO_2 electrodes was studied using **HRD**2 and **H**102 sensitizers relative to the standard **N**719. Although more or less similar absorption pattern with similar film absorption ratios on TiO_2 was observed, the change of dye bath from ethanol to acetonitrile/*tert*-butanol 1/1 v/v mixture has shown significant enhancement in photovoltaic performance. The variation in the solvents used in dye baths has influence on delivery of the dye molecules and the pattern of dye molecules sitting on the surface TiO_2 during the anchoring

phenomenon and ultimately lead to influence the overall light to electricity conversion efficiencies.

Acknowledgments

Ch. S. Rao thanks IICT-AIC collaborative project for a fellowship. M. Chandrasekharam thanks DST for the grant of the project entitled "Advancing the efficiency and production potential of Excitonic Solar Cells (APEX)" under UK-DST consortium. This paper is dedicated to Professor H. Junjappa on the eve of his 75th birth day.

References

[1] B. O'Regan and M. Grätzel, "A low-cost, high-efficiency solar cell based on dye-sensitized colloidal TiO_2 films," *Nature*, vol. 353, no. 6346, pp. 737–740, 1991.

[2] A. Hagfeldt, G. Boschloo, L. Sun, L. Kloo, and H. Pettersson, "Dye-sensitized solar cells," *Chemical Reviews*, vol. 110, no. 11, pp. 6595–6663, 2010.

[3] A. Hagfeld and M. Grätzel, "Light-induced redox reactions in nanocrystalline systems," *Chemical Reviews*, vol. 95, no. 1, pp. 49–68, 1995.

[4] K. Kalyanasundaram and M. Grätzel, "Applications of functionalized transition metal complexes in photonic and optoelectronic devices," *Coordination Chemistry Reviews*, vol. 177, no. 1, pp. 347–414, 1998.

[5] A. Hagfeldt and M. Grätzel, "Molecular photovoltaics," *Accounts of Chemical Research*, vol. 33, no. 5, pp. 269–277, 2000.

[6] M. Grätzel, "Dye-sensitized solar cells," *Journal of Photochemistry and Photobiology C*, vol. 4, no. 2, pp. 145–153, 2003.

[7] K. J. Jiang, N. Masaki, J. B. Xia, S. Noda, and S. Yanagida, "A novel ruthenium sensitizer with a hydrophobic 2-thiophen-2-yl-vinyl- conjugated bipyridyl ligand for effective dye sensitized TiO_2 solar cells," *Chemical Communications*, no. 23, pp. 2460–2462, 2006.

[8] Md. K. Nazeeruddin, C. Klein, P. Liska, and M. Grätzel, "Synthesis of novel ruthenium sensitizers and their application in dye-sensitized solar cells," *Coordination Chemistry Reviews*, vol. 249, no. 13-14, pp. 1460–1467, 2005.

[9] P. Wang, S. M. Zakeeruddin, J. E. Moser et al., "Stable new sensitizer with improved light harvesting for nanocrystalline dye-sensitized solar cells," *Advanced Materials*, vol. 16, no. 20, pp. 1806–1811, 2004.

[10] C.-Y. Chen, H.-C. Lu, C.-G. Wu, J.-G. Chen, and K.-C. Ho, "New ruthenium complexes containing oligoalkylthiophene-substituted 1,10-phenanthroline for nanocrystalline dye-sensitized solar cells," *Advanced Functional Materials*, vol. 17, no. 1, pp. 29–36, 2007.

[11] D. Martineau, M. Beley, P. C. Gros, S. Cazzanti, S. Caramori, and C. A. Bignozzi, "Tuning of ruthenium complex properties using pyrrole- and pyrrolidine-containing polypyridine ligands," *Inorganic Chemistry*, vol. 46, no. 6, pp. 2272–2277, 2007.

[12] Y. Xu, S. Sun, J. Fan, and X. Peng, "Tyrosine groups enhance photoinduced intramolecular electron transfer in polypyridyl ruthenium(II) complexes," *Journal of Photochemistry and Photobiology A*, vol. 188, no. 2-3, pp. 317–324, 2007.

[13] J. Faiz, A. I. Philippopoulos, A. G. Kontos, P. Falaras, and Z. Pikramenou, "Functional supramolecular ruthenium cyclodextrin dyes for nanocrystalline solar cells," *Advanced Functional Materials*, vol. 17, no. 1, pp. 54–58, 2007.

[14] M. K. Nazeeruddin, A. Kay, I. Rodicio et al., "Conversion of light to electricity by cis-X2bis(2,2′-bipyridyl-4,4′-dicarboxylate)ruthenium(II) charge-transfer sensitizers (X = Cl^-, Br^-, I^-, CN^-, and SCN^-) on nanocrystalline TiO_2 electrodes," *Journal of the American Chemical Society*, vol. 115, no. 14, pp. 6382–6390, 1993.

[15] C. J. Barbé, F. Arendse, P. Comte et al., "Nanocrystalline titanium oxide electrodes for photovoltaic applications," *Journal of the American Ceramic Society*, vol. 80, no. 12, pp. 3157–3171, 1997.

[16] M. K. Nazeeruddin, P. Péchy, T. Renouard et al., "Engineering of efficient panchromatic sensitizers for nanocrystalline TiO_2-based solar cells," *Journal of the American Chemical Society*, vol. 123, no. 8, pp. 1613–1624, 2001.

[17] C. Klein, Md. K. Nazeeruddin, D. Di Censo, P. Liska, and M. Grätzel, "Amphiphilic ruthenium sensitizers and their applications in dye-sensitized solar cells," *Inorganic Chemistry*, vol. 43, no. 14, pp. 4216–4226, 2004.

[18] H. Sugihara, L. P. Singh, K. Sayama, H. Arakawa, M. K. Nazeeruddin, and M. Grätzel, "Efficient photosensitization of nanocrystalline TiO_2 films by a new class of sensitizer: cis-dithiocyanato bis(4,7-dicarboxy-1,10-phenanthroline)ruthenium(II)," *Chemistry Letters*, no. 10, pp. 1005–1006, 1998.

[19] T. Renouard, R. A. Fallahpour, M. K. Nazeeruddin et al., "Novel ruthenium sensitizers containing functionalized hybrid tetradentate ligands: synthesis, characterization, and INDO/S analysis," *Inorganic Chemistry*, vol. 41, no. 2, pp. 367–378, 2002.

[20] P. Wang, C. Klein, R. Humphry-Baker, S. M. Zakeeruddin, and M. Grätzel, "A high molar extinction coefficient sensitizer for stable dye-sensitized solar cells," *Journal of the American Chemical Society*, vol. 127, no. 3, pp. 808–809, 2005.

[21] M. Chandrasekharam, C. Srinivasarao, T. Suresh et al., "High spectral response heteroleptic ruthenium (II) complexes as sensitizers for dye sensitized solar cells," *Journal of Chemical Sciences*, vol. 123, no. 1, pp. 37–46, 2011.

[22] M. Chandrasekharam, G. Rajkumar, Ch. S. Rao, T. Suresh, and P. Y. Reddy, "Phenothiazine conjugated bipyridine as ancillary ligand in Ru(II)-complexes for application in dye sensitized solar cell," *Synthetic Metals*. In press.

[23] P. Y. Reddy, L. Giribabu, C. Lyness et al., "Efficient sensitization of nanocrystalline TiO_2 films by a near-IR-absorbing unsymmetrical zinc phthalocyanine," *Angewandte Chemie—International Edition*, vol. 46, no. 3, pp. 373–376, 2007.

[24] L. Giribabu, M. Chandrasekheram, M. L. Kantham et al., "Conjugated organic dyes for dye-sensitized solar cells," *Indian Journal of Chemistry. Section A*, vol. 45, no. 3, pp. 629–634, 2006.

[25] M. Chandrasekharam, G. Rajkumar, C. Srinivasa Rao et al., "Polypyridyl Ru(II)-sensitizers with extended π-system enhances the performance of dye sensitized solar cells," *Synthetic Metals*, vol. 161, no. 11-12, pp. 1098–1104, 2011.

[26] M. Chandrasekharam, G. Rajkumar, Ch. S. Rao, T. Suresh, and P. Y. Reddy, "Ruthenium(II)- bipyridyl with extended π-system: improved thermo-stable sensitizer for efficient and long-term durable dye sensitized solar cells," *Journal of Chemical Sciences*. In press.

[27] L. Giribabu, C. Vijay Kumar, C. S. Rao et al., "High molar extinction coefficient amphiphilic ruthenium sensitizers for efficient and stable mesoscopic Dye-sensitized solar cells," *Energy and Environmental Science*, vol. 2, no. 7, pp. 770–773, 2009.

[28] H. Tian, X. Yang, R. Chen, R. Zhang, A. Hagfeldt, and L. Sun, "Effect of different dye baths and dye-structures on the performance of dye-sensitized solar cells based on triphenylamine dyes," *Journal of Physical Chemistry C*, vol. 112, no. 29, pp. 11023–11033, 2008.

[29] J.-J. Cid, J.-H. Yum, S.-R. Jang et al., "Molecular cosensitization for efficient panchromatic dye-sensitized solar cells," *Angewandte Chemie—International Edition*, vol. 46, no. 44, pp. 8358–8362, 2007.